www.ietdl.org

Published in IET Computer Vision
Received on 2nd March 2012
Revised on 17th August 2012
doi: 10.1049/iet-cvi.2012.0044

ISSN 1751-9632

Empirical investigation into the correlation between vignetting effect and the quality of sensor pattern noise

C.-T. Li[1] *R. Satta*[2]

[1]*Department of Computer Science, University of Warwick, Coventry CV4 7AL, UK*
[2]*Department of Electrical and Electronic Engineering, University of Cagliari, Cagliari 09123, Italy*
E-mail: c-t.li@warwick.ac.uk

Abstract: The sensor pattern noise (SPN) is a unique attribute of the content of images that can facilitate identification of source digital imaging devices. Owing to its potential in forensic applications, it has drawn much attention in the digital forensic community. Although much work has been done on the applications of the SPN, investigations into its characteristics have been largely overlooked in the literature. In this study, the authors aim to fill this gap by providing insight into the characteristic dependency of the SPN quality on its location in images. They have observed that the SPN components at the image periphery are not reliable for the task of source camera identification, and tend to cause higher false-positive rates. Empirical evidence is presented in this work. The authors suspect that this location-dependent SPN quality degradation has strong connection with the so-called 'vignetting effect', as both exhibit the same type of location dependency. The authors recommend that when image blocks are to be used for forensic investigations, they should be taken from the image centre before SPN extraction is performed in order to reduce false-positive rate.

1 Introduction

Attributed to the combined effect of falling prices and increased functionalities, digital imaging devices are as common as watches and wallets in our everyday life in the past two decades. Multimedia manipulations have been made easy with the availability of powerful and easy-to-use multimedia processing software. This has undoubtedly opened up many new opportunities and possibilities for positive purposes. However, the very same set of technologies also provides means for malicious intention to be realised. In response to the challenges posed by the abuse of these technologies, 'multimedia forensics' has emerged as a new and fast-evolving discipline with the aim of undertaking combat against digital crime. Typical 'multimedia forensic' applications include source device identification [1–4], source device linking [5], classification of images taken by unknown cameras [6–8], content integrity verification and authentication [7, 9] etc.

At the centre of these technologies and applications is digital imaging devices, especially digital cameras, and the content they produce. It is therefore useful to have a closer look at how a typical digital camera works and how it produces images. Fig. 1 illustrates the simplified digital image acquisition process that a typical digital camera has to go through in order to produce a photo. The light emitting from the scene enters the lens, passes through an anti-aliasing filter, and then reaches a colour filter array (CFA) that is recurrently placed over the semiconductor sensors to capture colour information. Each element of the CFA is only sensitive to a certain light wavelength range such that the corresponding sensor pixel receives only one of the red (R), green (G) and blue (B) components of the light. The missing two colours at each pixel are subsequently interpolated by a de-mosaicking process based on the colour configuration within a neighbourhood of the pixel in question. A sequence of image processing operations, such as colour correction, white balancing, Gamma correction, enhancement and JPEG compression, then take place before the photo is stored in the disk. At each stage of the acquisition pipeline, the hardware and software involved may leave unique 'fingerprints' in the content of the image, which can be exploited to identify the imaging devices. Therefore researchers have proposed a number of techniques to extract such fingerprints from images for various forensic investigation purposes. Modalities among the fingerprints that have drawn much attention from scientists are sensor pattern noise (SPN) [1, 2, 4–6, 9, 10], camera response function [11, 12], CFA interpolation artefacts [13, 14], traces of sensor dust [15], JPEG compression [16] and lens aberrations [17, 18].

Although many methods [10, 11, 13, 14] can only be applicable when specific assumptions or constraints are satisfied, the SPN has attracted much greater interest because of its independence of the similar assumptions and constraints. Another desirable feature of the SPN is that it can not only identify camera models, but also individual

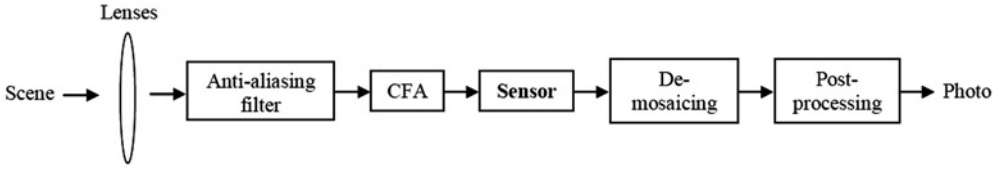

Fig. 1 *Process of image acquisition that takes place in a typical digital camera*

cameras of the same model [1, 2, 4, 9, 19]. This desirable characteristic of SPN is ironically attributed to manufacturing imperfections and different sensitivity of pixels to light because of the inhomogeneity of silicon wafers [20]. However, the uniqueness of manufacturing imperfections and the non-uniform sensitivity of each pixel to the light, even sensors made from the same silicon wafer would produce uncorrelated and unique pattern noise, which is not visible to human eyes. The reader is referred to [20] for more details in relation to the SPN. Owing to its potential in forensic applications, SPN has drawn much attention in the digital forensic community. Although much work has been done on the applications of the SPN [1–4, 6, 7, 9, 19], investigations into its characteristics have been largely overlooked in the literature. This has motivated this work and its previous preliminary study [21]. By providing insight into the characteristic dependency of the SPN quality on its location in images, we aim to fill the gap between SPN applications and SPN characteristics in order to avoid the undesirable SPN characteristics in its real-world applications.

In [21], we focused on studying an anomaly in the changes of false-positive rates with respect to the size of image blocks in source device identification, when two SPN-based methods reported in [1] and [2] are used. Our findings suggested that this anomaly may well be because of the so-called 'vignetting effect', because it exhibits a similar location-dependent characteristic as the quality of the SPN. In this work, we extend the empirical investigation of [21] with two new contributions. Firstly, we evaluate the effective location dependency of the quality of SPN, by measuring the similarity of SPN from different cameras, when they are taken from changing locations of the image. Secondly, we evaluate the impact of such location dependency in the performance attained by the method of [1] in the task of source camera identification. We point out that the aim of the latter analysis is similar to that of [21]. However, in [21] our investigations involved only a small set of clear sky images without any high-frequency details because we would like to assess the SPN location-dependent quality without the influence of scene details. Instead, in this work we use a bigger dataset containing images of various scenes, both indoor and outdoor, in order to evaluate the influence of the location dependency of SPN quality in a more realistic setting. In addition, in [21] we considered only a small subset of locations of the block from which the SPN is extracted, whereas in this work we consider all the possible locations with an exhaustive analysis.

The rest of this work is organised as follows. We first review two SPN-based source device identification methods [1, 2] in Section 2. The anomaly is then discussed in Section 3. In Section 4, we provide a brief insight into the vignetting effect. Empirical investigations into the location-dependent quality of SPN are presented in Section 5. Finally, conclusions and further research directions are drawn in Section 6.

2 Previous work

Most SPN-based image forensic techniques [2, 4, 5, 8, 9, 19] extract the SPN by exploiting the additive noise model in [1] or its variant [5]. Denoting n as the SPN in an image I, the model proposed in [1] [when used in the discrete wavelet transform (DWT) domain] can be formulated as

$$n = \mathrm{DWT}(I) - F(\mathrm{DWT}(I)) \tag{1}$$

where DWT is the discrete wavelet transform and F is a de-noising filter. Owing to the high-frequency nature of the SPN, F is usually a low-pass filter. Subtracting the de-noised version of I from the original version leaves the high-frequency components of I to be used as the SPN, n. As one can easily see, the de-noising function F plays a major role in determining the reliability of SPN. Although different de-noising filters can be used as F, the wavelet-based de-noising filter presented in the Appendix A of [1] has been known as effective in producing good results. As such, it is used in this work.

Once SPN is extracted, it can be used in a variety of forensic applications, for instance identifying the source camera of an image [1–4, 19], clustering images according to their source devices [6] and content integrity verification [9]. To these ends, a metric for evaluating the similarity between SPNs is necessary. A common distance metrics for measuring the similarity between the SPNs n_i and n_j of images i and j is the normalised cross-correlation defined as

$$\rho(i,j) = \frac{(n_i - \bar{n}_i)\cdot(n_j - \bar{n}_j)}{\|n_i - \bar{n}_i\| \cdot \|n_j - \bar{n}_j\|} \tag{2}$$

where $\bar{n}_i$ and $\bar{n}_j$ are the means of n_i and n_j, respectively. In source device identification, n_j is a template SPN, usually obtained by averaging different SPNs extracted from a number of images taken by the same device. If the similarity $\rho(i,j)$ is greater than a given threshold, image i is classified as taken by device j. A commonly adopted threshold is 0.01 [1, 2, 5, 7, 9].

A challenging issue that affects the quality and reliability of SPN is the presence of edges and details in the scene, for example, brick walls, tree leaves and other types of textured surfaces. Such details appear as high-frequency components in the DWT domain of the image, whose magnitude is typically greater than that of SPN by many orders of magnitude, thus distorting the quality of the extracted SPN. Fig. 2 illustrates a good example. Fig. 2*a* is an image without details and Fig. 2*b* is the SPN extracted from Fig. 2*a* using the method of [1]. Since there is no significant details in Fig. 2*a*, the intensity of the extracted SPN is minute. However, if the image contains siginficant details such as Fig. 2*c*, the extracted SPN, as shown in Fig. 2*d*, will contain those details (i.e. the SPN is contaminated by those details). Therefore forensic

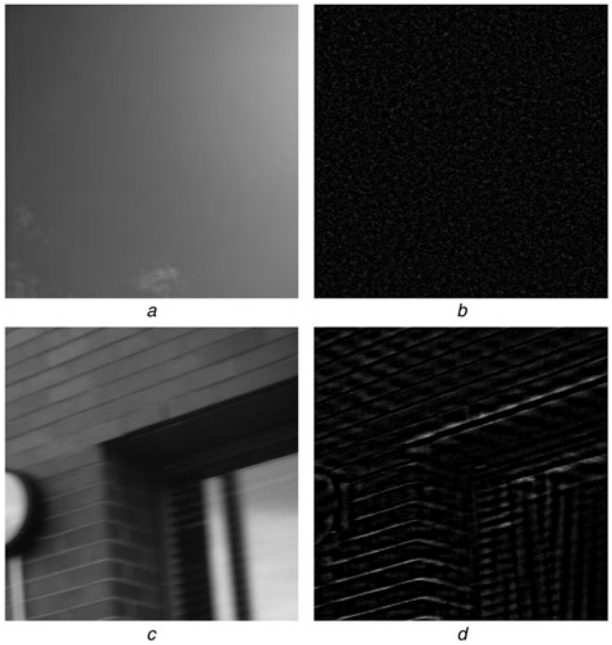

Fig. 2 *Quality and reliability of SPN*

a Image without details
b SPN extracted from *a*
c Image with significant details
d SPN extracted from *c*

investigations based on contaminated SPNs are likely to be questionable. We addressed this issue in a previous work [2] using an effective SPN enhancer that attenuates the interference of scene details. The enhancer is based on the underlying hypothesis that strong SPN signal components are not trustworthy, as it is more likely that they are created by high-frequency details. Following this hypothesis, an enhanced SPN can be obtained by assigning weighting factors inversely proportional to the magnitude of the signal components. The reader is referred to [2] for further details about the SPN enhancer.

3 Anomaly reported in previous work

Matching two SPNs through (2) can be performed by considering only a block of the image, for example a block of 256 × 256 or 512 × 512 pixels. Using bigger blocks leads to higher performance, whereas the use of smaller blocks reduces the computational complexity and speeds up the matching process. In [2], the performance of the SPN enhancer was compared to that of the method in [1] in the task of source camera identification, with various block sizes considered. On one hand, results reported in [2] confirm the effectiveness of the SPN enhancer-based approach and its superiority to the method in [1]. On the other hand, both methods show an anomaly in the changes of false-positive rates with respect to block sizes (see Table 1). Table 1 reports the device identification performance of both methods. We use M1 to stand for the method of [1] and M2 to stand for our proposed SPN enhancer [2]. It can be seen that the false-positive rate initially decreases as the size of the image block is greater, reaches the minimum when the block size is 1024 × 1024 pixels, then increases significantly afterwards. This anomaly (i.e. the decreasing false-positive rates with respect to the decreasing block size when the blocks sizes are greater than 1024 × 1024 pixels) is particularly clearer for the case without enhancement (i.e. M1). After applying other values of the similarity threshold (0.005, 0.015, 0.02, 0.025 and 0.03), we still observed the same anomaly.

We could not explain the cause of this anomaly at the time of writing [2]. However, our recent study into the 'vignetting effect' (i.e. reduction of brightness at the peripheral areas of images) in optics and photography [20–24] has pointed us to the possibility that vignetting may have a role in distorting the SPN in a location-dependent manner. Our experiments, to be presented in Section 5, reveal that source camera identification based on SPN blocks taken from locations near the centre of the image produce lower false-positive rates, whereas blocks from the periphery lead to significantly higher false-positive rates. This fact has confirmed that the quality of the SPN exhibits the similar location-dependent characteristic as that of the vignetting effect. Although without further in-depth research, it is difficult to definitely conclude that such a location-dependent SPN quality variation is due to the vignetting effect, we would like to

1. present our finding of this location-dependency of SPN quality and
2. recommend that the image borders be avoided if only portions/blocks of the full-size images are needed for forensic applications.

We also hope that this work will facilitate further discussions over the possible connection between the vignetting effect and the location-dependent SPN quality degradation in order to gain better understanding of SPN characteristics. A brief review of the vignetting effect is presented in the next section.

4 Vignetting

Vignetting is the location-dependent reduction of brightness in optics and photography at the peripheral areas of photos.

Table 1 False-positive rates with (M2) and without (M1) applying the SPN enhancer of [2] to the SPNs extracted with the model proposed in [1]

Method	False-positive rate (%) associated with blocks of various sizes								
	128 × 128	128 × 256	256 × 256	256 × 512	512 × 512	512 × 1024	1024 × 1024	1024 × 2048	1536 × 2048
M1	41.68	38.68	32.60	25.71	16.28	6.75	1.90	2.40	12.03
M2	8.33	3.22	0.95	0.15	0.03	0	0	0.03	0.4

Note that in this experiment, the image is deemed as taken by the cameras that are not the source camera if their similarity values are greater than a threshold 0.01. The photos contain a variety of natural indoor and outdoor scenes taken during holidays, around campus and cities, in offices and laboratories etc

doi: 10.1049/iet-cvi.2012.0044

Fig. 3 *Image affected by vignetting effect*
Brightness at the centre of the image is greater than that at the periphery

Brightness is higher in the centre of the images and falls off gradually towards the edges (see Fig. 3 for an example). Vignetting can often be seen in photographic portraits that usually are clearer in the centre and fade off at the periphery. It may also be added in post-production, as it is perceived as pleasant in certain kinds of photographs. However, camera settings and lens design are the main physical causes of the vignetting effect. Four main types of vignetting exist, each because of a different reason [23]:

- *Optical vignetting:* This type of vignetting is inherent in the lens design and is due to the physical aperture of a multiple element lens. As the lens has a length, the on-axis light from the scene (corresponding to the image centre) impinges the lens spot-on, whereas the off-axis light (corresponding to image periphery) may be blocked by the lens body. As a result, the effective entrance pupil for the off-axis incident light is reduced, making the image edges appear darker than the image centre.
- *Natural vignetting:* Also known as natural illumination falloff, natural vignetting is caused by the different angles at which the light strikes on different locations of the sensor array. The path from the rear end of the lens (the exit pupil) to the edges of the sensor is longer than to the centre of the sensor. Therefore light has to travel longer. The longer the journey is, the greater the loss of light intensity. According to the so-called 'cosine fourth' law of illumination falloff, the loss of intensity is proportional to $\cos^4 \theta$, where θ is the angle of the incident light on the sensor array. With a zoom lens, the natural vignetting effect is generally inversely proportional to the focal length.
- *Pixel vignetting:* It is caused by the differences in the incident angle of the photons in respect to pixels sensor elements. Photons striking perpendicularly on a sensor element produce stronger signals than photons hitting it at an oblique angle. This angle dependence of the sensor response also contributes to the falloff of brightness towards the edges of images.
- *Mechanical vignetting:* This is due to the use of inappropriate attachments to the lens, such as thick or stacked filters, secondary lenses and misaligned lens hoods that partially block the light path.

Based on the above discussions, we can see that both vignetting effect and false-positive device identification rates increase with respect to the distance of the sensor elements/image pixels from the centre of images. As such, we expect that the vignetting effect is likely to be the cause (or one of the main causes) of the location-dependent SPN quality variation.

5 Empirical investigations

We conducted a series of experimental investigations to assess: (i) the location dependency of SPN quality and (ii) its implications in a practical task: source camera identification. The results are presented in Sections 5.1 and 5.2, respectively. Note that as we can see from Table 1, the anomalous changes of false-positive rates are more evident when M1 is applied and thus can better facilitate our discussions. Therefore we will use M1 in our experiments to extract the SPN.

5.1 Location-dependent quality of SPN

In the first set of experiments, we evaluated the 'inter-camera' (i.e. 'inter-class') similarity of the SPN with respect to the location of the block from which the SPN is obtained. The rationale behind this set of experiments is that higher-quality SPNs should exhibit a lower 'inter-camera' similarity, that is, they should be more different from each another.

To analyse the quality of SPN without the influence of scene details, we used 300 photos of blue sky in JPEG format taken by six different cameras, each responsible for 50. The JPEG quality factors of the images range approximately from 93 to 97%. The six cameras (C_1–C_6) are Canon IXUS 850IS, Canon PowerShot A400, Canon IXY Digital 500, FujiFilm A602, FujiFilm FinePix A902 and Olympus FE210. The sizes of the images of all the cameras are 1536×2048 pixels. The SPN of each camera was obtained as the average of 50 SPN, each from one image taken by the camera.

We divide each image into 192 ($=12 \times 16$) non-overlapping blocks of 128×128 pixels. We then extracted the SPN from each block. For each camera C_i, and for each block location in the grid, we evaluated the average similarity between the SPN block extracted from C_i and the SPN block extracted from the other cameras C_j, $j \neq i$. The similarity between SPN blocks was obtained via the normalised cross-correlation of (2). The average SPN similarity with respect to the block position is shown in Fig. 4 for all the cameras. In Fig. 5, we also show the average inter-camera similarity with respect to the block position, as the average of the six plots in Fig. 4.

As can be seen from Figs. 4 and 5, the SPN similarity shows a noticeable location-dependent behaviour. In particular, the average similarity between the SPN of different cameras tends to be higher when SPN blocks are taken near the borders, whereas it goes lower moving towards the centre of the image; in other words, the SPN tend to loose its 'uniqueness' in peripheral locations of the image. This behaviour suggests that the SPN quality is distorted in a manner similar to the change of brightness of images because of vignetting effect as shown in Fig. 3. The degradation is particularly evident in the corners, where the highest inter-camera similarities are attained. This is consistent to our hypothesis that the location-dependent quality of SPN is caused by the vignetting effect, as the corners are the most affected locations of the image with respect to vignetting. Note that the inter-camera similarity of camera C_6 shows a different behaviour, in fact, this camera shows low inter-camera similarities even in the borders, with the exception of

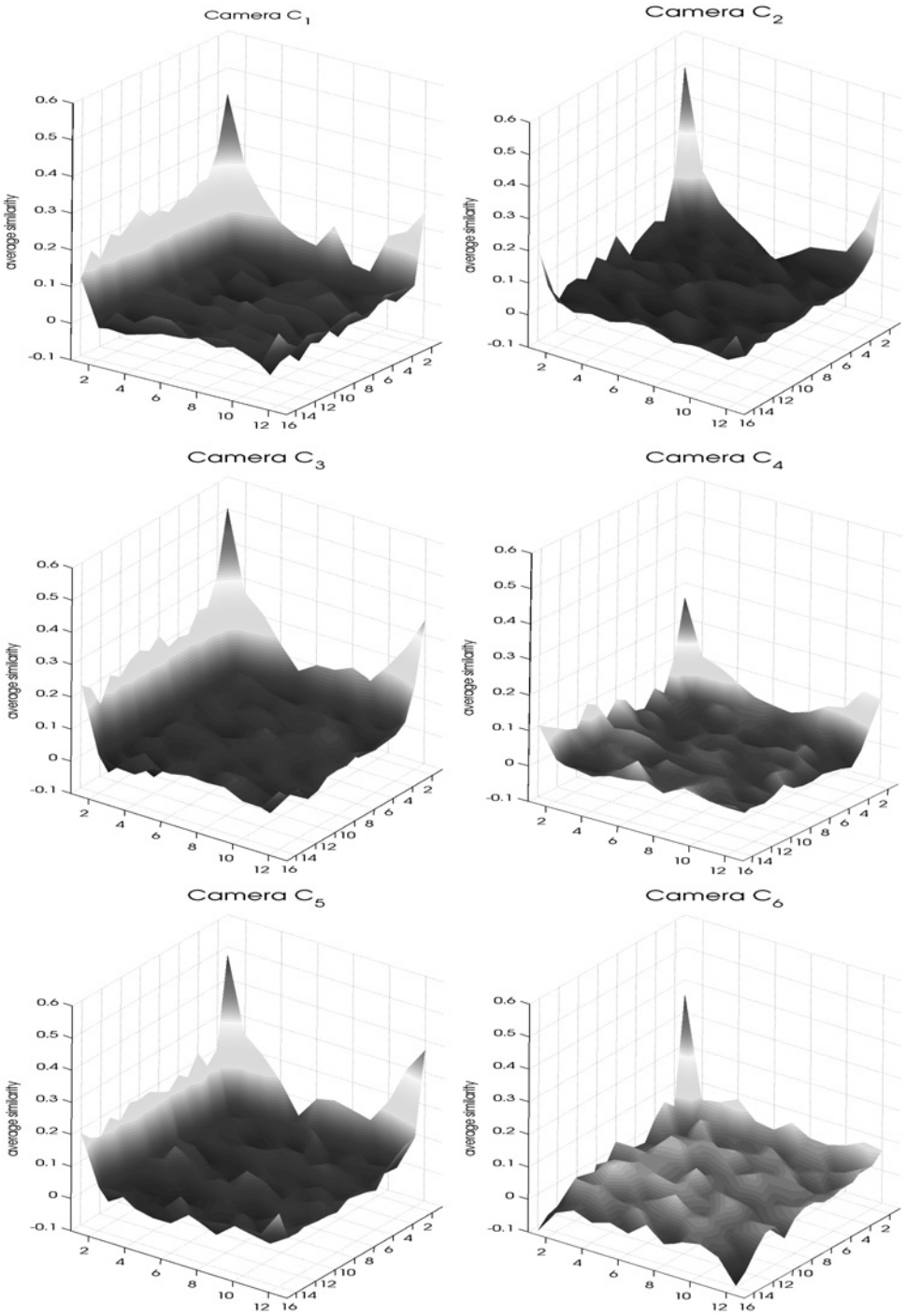

Fig. 4 *Average SPN similarity with respect to the block position for all cameras*

the 'upper-left' corner. This is most probably because of a better constructive quality that possibly allows C_6 to handle vignetting better than the other cameras.

It is worth noting that on an average, the inter-camera similarity (Fig. 5) is higher in the 'upper' and 'left' borders than in the 'lower' and 'right' ones (see Table 2, which shows the average inter-camera SPN similarity in the four borders), and the maximum in the upper corners. This suggests that the quality degradation of the SPN components is asymmetrical with respect to the centre of the image. Thus, the SPN quality does not necessarily vary isotropically.

The location-dependent behaviour shown above is likely to impact in all the forensics tasks involving SPN. In the next section, we focus on the influence of the SPN block location in the task of [2] that is, source camera identification.

5.2 Impact of SPN location dependency in source camera identification

Following the first set of experiments of Section 5.1, in this section we evaluate the impact of the location-dependent behaviour of SPN quality, in the task of source camera identification [1, 2, 5, 7, 9]. We used the same six cameras of Section 5.1, and the same 300 photos, to extract a reference SPN block n_c of each camera c. As in Section 5.1, the reference SPN of each camera was obtained by averaging 50 SPN, each from one image taken by the

doi: 10.1049/iet-cvi.2012.0044

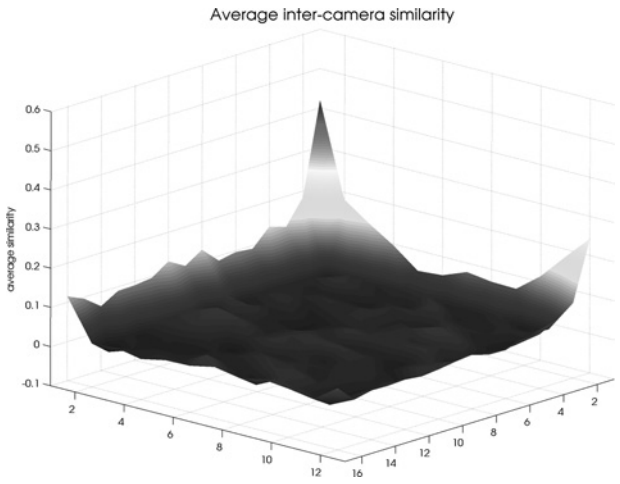

Fig. 5 *Average inter-camera similarity, measured in terms of normalised cross-correlation, of the SPN, as a function of the SPN block position*

x- and *y*-axes represent the block position with respect to a 12 × 16 regular grid used to subdivide the image

camera. We then extracted an SPN block n_i from each image i of a different data set of 1200 photos, taken by the same six cameras (each camera was responsible of 200 photos). These images contain various indoor and outdoor scenes and were shot at different hours of the day. The normalised cross-correlation defined in (3) was used to measure the similarity between SPNs n_i of images i and the reference SPNs n_c

$$\rho(i, c) = \frac{(n_i - \bar{n}_i) \cdot (n_c - \bar{n}_c)}{\|n_i - \bar{n}_i\| \cdot \|n_c - \bar{n}_c\|}, \quad c \in (1, 6) \tag{3}$$

where $\bar{n}_i$ and $\bar{n}_c$ are the means of n_i and n_c, respectively. For each image block, if its similarity with any camera's reference SPN block was greater than 0.01, this image was deemed as taken by the camera. Note that each image could be labelled as taken by more than one camera depending on $\rho(i, c)$.

Similarly to the experiments of Section 5.1, we changed the location at which the reference SPNs blocks n_c and the probe SPNs n_i blocks were extracted, by means of a regular grid. We carried out two experiments. In the first experiment (denoted as EXP_512 in the following), we used a block of size 512 × 512 pixels, and moved the block from left to right and from top to bottom, with a displacement of 64 pixels. In total, 425 (=17 × 25) different blocks were cropped. In the second experiment (denoted as EXP_256 in the following), we set the block size to 256 × 256 pixels and the displacement step to 32 pixels. In total, 2337 (41 × 57) different blocks are obtained from different locations.

In both experiments EXP_512 and EXP_256, for each block position, we evaluated the source camera identification performance. In particular, we measured the

Table 2 Average inter-camera similarity of SPN in the four image borders and in the image centre

Average SPN similarity (normalised cross-correlation)				
Upper border	Left border	Lower border	Right border	Centre
0.1278	0.1404	0.0498	0.0301	0.0047

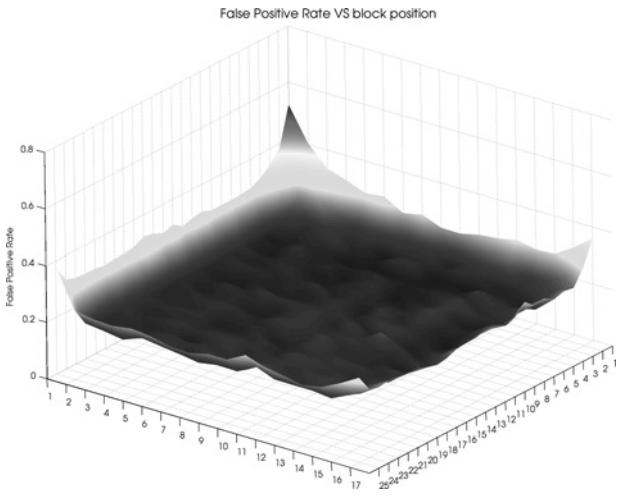

Fig. 6 *EXP_512: false-positive rate as a function of the position at which the SPN block is extracted, with respect to a 17 × 25 regular grid, and blocks of 512 × 512 pixels*

false-positive rate (i.e. the percentage of incorrect assignments), since the anomaly reported in Section 3 affected the number of false positives. The false-positive rates with respect to the block position at which the SPN is extracted are shown in Figs. 6 and 7 for EXP_512 and EXP_256, respectively. As one can easily see, the same location-dependent behaviour that affects the inter-camera similarity of SPN (see Figs. 4 and 5) arises in camera identification performance. This again demonstrates the close relationship between the vignetting effect and SPN quality.

The above results have conformed to our expectation that the SPN quality is indeed location-dependent and it is degradated to a greater extent at the image periphery. Furthermore, we showed that this behaviour influences the performance of source camera identification. As such, we can conclude that

- This explains the anomaly reported in Table 3 of [2] (duplicated as Table 1 in this work). When full-size images (1536 × 2048 pixels) are used for device identification, although more data are involved to help with the

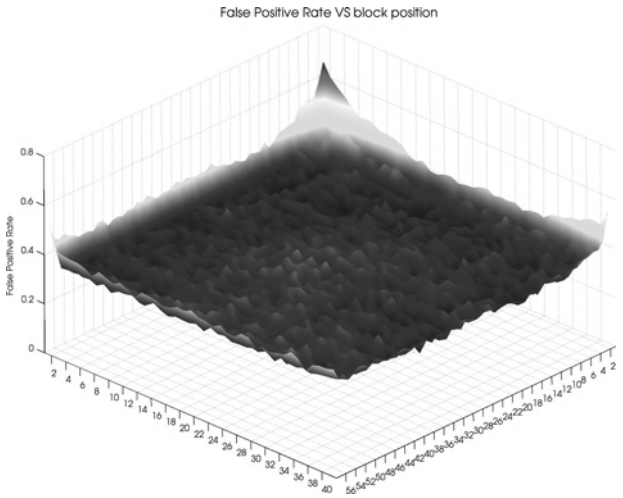

Fig. 7 *EXP_256: false-positive rate as a function of the position at which the SPN block is extracted, with respect to a 41 × 57 regular grid, and blocks of 256 × 256 pixels*

identification, the SPN components of poor quality along the image borders are also included, which out-weigh the benefit of using the whole image. By comparing the figures in Table 1, we can see that when only blocks of 1024 × 2048 pixels taken from the image centre are used, the false-positive rate drops from 12.03 (when the full-size images are use) to 2.4%. This is because the 256 rows at the top edge and the 256 rows at the bottom edges have been excluded. Hence, even though only 66.67% (=1024/1536) of the original pixels are used, the exclusion of the SPN components of poorer quality at the periphery allows better performance to be gained. This trend continues as the blocks size is further reduced down to 1024 × 1024. This time not only the 512 rows at the periphery, but also the 1024 columns at the image periphery are excluded. However, when the block size is further reduced down to 512 × 1024, the false-positive rates start to increase, indicating that the SPN components of poor quality have been sufficiently excluded and the identifier is starting to suffer from the lack of useful data (i.e. SPN components of better quality).

- In forensic applications wherein smaller image blocks are required (e.g. blind classification of large image datasets [6–8]), it is advisable that blocks are taken from the image centre.

6 Conclusions

SPN carries a high potential in digital forensic applications. Therefore it is important to better understand its characteristics and their impact on the accuracy of the information/evidence drawn from forensic analysis. In a previous work, we observed a counter intuitive situation that full-size images or image blocks closer to the image periphery tend to give rise to higher false-positive rates when used for source camera identification. In this work, starting with the assumption that this anomaly might be related to the vignetting effect because of the lens/sensor design and/or camera settings, we have carried out a series of experiments to see if significant performance discrepancy can be found when the SPN from peripheral blocks and inner blocks are used. The experiments have confirmed that, like the vignetting effect, the SPN quality is indeed location dependent and explained the cause of the anomaly. Based on the experimental results, our recommendations for the digital forensics communities are

- excluding the peripheral pixels of images before the SPN is extracted for source camera identification and linking;
- taking the blocks from the centre when only small blocks are needed in the applications (e.g. image classification);
- exercising cautions when dealing with blocks along the image periphery, when block-based integrity verification is to be carried out.

It is our aim in this work to facilitate further discussions and in-depth study into the characteristics of the SPN. Our future work will include a more thorough investigation into the relationship between the vignetting effect and SPN quality, as well as devising models and methods to quantitatively assess the quality of the components of SPN.

7 References

1 Lukáš, J., Fridrich, J., Goljan, M.: 'Digital camera identification from sensor pattern noise', *IEEE Trans. Inf. Forensics Sec.*, 2006, **1**, (2), pp. 205–214
2 Li, C.-T.: 'Source camera identification using enhanced sensor pattern noise', *IEEE Trans. Inf. Forensics Sec.*, 2010, **5**, (2), pp. 280–287
3 Khanna, N., Delp, E.J.: 'Source scanner identification for scanned documents'. Proc. IEEE Int. Workshop on Information Forensics and Security, London, UK, December 2009, pp. 166–170
4 Caldelli, R., Amerini, I., Picchioni, F., De Rosa, A., Uccheddu, F.: 'Multimedia forensic techniques for acquisition device identification and digital image authentication', in Li, C.-T. (Ed.): 'Handbook of research on computational forensics, digital crime and investigation: methods and solutions' (Information Science Reference, IGI Global, 2009), pp. 130–154
5 Fridrich, J.: 'Digital image forensic using sensor noise', *IEEE Signal Process. Mag.*, 2009, **26**, (2), pp. 26–37
6 Li, C.-T.: 'Unsupervised classification of digital images using enhanced sensor pattern noise'. Proc. IEEE Int. Symp. Circuits and Systems (ISCAS'10), Paris, France, May 2010, pp. 3429–3432
7 Caldelli, R., Amerini, I., Picchioni, F., Innocenti, M.: 'Fast image clustering of unknown source images'. Proc. IEEE Int. Workshop on Information Forensics and Security, Seattle, USA, December 2010
8 Liu, B.-B., Lee, H.-K., Hu, Y., Choi, C.-H.: 'On classification of source cameras: a graph based approach'. Proc. IEEE Int. Workshop on Information Forensics and Security, Seattle, USA, December 2010, pp. 1–5
9 Li, C.-T., Li, Y.: 'Colour-decoupled photo response non-uniformity for digital image forensics', *IEEE Trans. Circuits Syst. Video Technol.*, 2012, **22**, (2), pp. 260–271
10 Gou, H., Swaminathan, A., Wu, M.: 'Intrinsic sensor noise features for forensic analysis on scanners and scanned images', *IEEE Trans. Inf. Forensics Sec.*, 2009, **4**, (3), pp. 476–491
11 Hsu, Y.-F., Chang, S.-F.: 'Camera response functions for image forensics: an automatic algorithm for splicing detection', *IEEE Trans. Inf. Forensics Sec.*, 2010, **5**, (4), pp. 816–825
12 Ng, T.-T., Tsui, M.-P.: 'Camera response function signature for digital forensics - part I: theory and data selection'. Proc. IEEE Int. Workshop on Information Forensics and Security, London, UK, December 2009, pp. 156–160
13 Popescu, A.C., Farid, H.: 'Exposing digital forgeries in color filter array interpolated images', *IEEE Trans. Signal Process.*, 2005, **53**, (10), pp. 3948–3959
14 Cao, H., Kot, A.C.: 'Accurate detection of demosaicing regularity for digital image forensics', *IEEE Trans. Inf. Forensics Sec.*, 2009, **4**, (4), pp. 899–910
15 Dirik, A.E., Sencar, H.T., Memon, N.: 'Digital single lens reflex camera identification from traces of sensor dust', *IEEE Trans. Inf. Forensics Sec.*, 2008, **3**, (3), pp. 539–552
16 Huang, F., Huang, J., Shi, Y.H.: 'Detecting double JPEG compression with the same quantization matrix', *IEEE Trans. Inf. Forensics Sec.*, 2010, **5**, (4), pp. 848–856
17 Lanh, V.T., Emmanuel, S., Kankanhalli, M.S.: 'Identifying source cell phone using chromatic aberration'. Proc. IEEE Conf. Multimedia and Expo, Beijing, China, July 2007, pp. 883–886
18 Choi, K.S., Lam, E.Y., Wong, K.K.Y.: 'Automatic source camera identification using the intrinsic lens radial distortion', *Opt. Express*, 2006, **14**, (24), pp. 11551–11565
19 Kang, X., Li, Y., Qu, Z., Huang, J.: 'Enhancing source camera identification performance with a camera reference phase sensor pattern noise', *IEEE Trans. Inf. Forensics Sec.*, 2012, **7**, (2), pp. 393–402
20 Janesick, J.R.: 'Scientific charge-coupled devices' (SPIE, vol. PM83, Bellingham, USA, 2001)
21 Li, C.-T., Satta, R.: 'On the location-dependent quality of the sensor pattern noise and its implication in multimedia forensics'. Proc. Fourth Int. Conf. Imaging for Crime Detection and Prevention (ICDP 2011), London, UK, November 2011, pp. 1–6
22 Hecht, H.: 'Optics' (Addison-Wesley, 2002)
23 Ray, S.F.: 'Applied photographic optics' (Focal Press, 2002, 3rd edn.)
24 Goldman, D.B., Chen, J.-H.: 'Vignette and exposure calibration and compensation'. Proc. IEEE Int. Conf. Computer Vision, Beijing, China, October 2005, vol. 1, pp. 899–906

doi: 10.1049/iet-cvi.2012.0044